ISSN 1392–1320 MATERIALS SCIENCE (MEDŽIAGOTYRA). Vol. 21, No. 3. 2015

Surface Modification of Austenitic Steel by Various Glow-Discharge Nitriding Methods

Tomasz BOROWSKI *, Bogusława ADAMCZYK-CIEŚLAK, Agnieszka BROJANOWSKA, Krzysztof KULIKOWSKI, Tadeusz WIERZCHOŃ

Warsaw University of Technology, Faculty of Materials Science and Engineering, ul. Woloska 141, 02-507 Warsaw, Poland

crossref http://dx.doi.org/10.5755/j01.ms.21.3.7404

Received 22 June 2014; accepted 21 December 2014

The article presents a characterisation of nitrided layers produced on austenitic X2CrNiMo17-12-2 (AISI 316L) stainless steel in the course of glow-discharge nitriding at cathodic potential, at plasma potential, and at cathodic potential incorporating an active screen. All processes were carried out at 440 °C under DC glow-discharge conditions and in 100 kHz frequency pulsed current. The layers were examined in terms of their microstructure, phase and chemical composition, morphology, surface roughness, hardness, wear, and corrosion resistance. Studies have shown a strong influence of the type of nitriding method used and of the electrical conditions on the microstructure and properties of the diffusion layers formed.

Keywords: glow-discharge nitriding, active screen, plasma and cathodic potential, DC and pulsating current, austenitic steel.

1. INTRODUCTION

Recently, a number of studies have been conducted concerning the use of an active screen in glow-discharge treatment, where the processed component is electrically insulated from the cathode, and its heat-up is carried out by means of heat convection originating in the active screen, on which cathodic glow is generated [1]. This is a forward-looking technology, as it allows for a uniform layer to be formed on the entire surface of the component, without the so-called edge effect, which occurs in classical methods of treatment employing glow-discharge nitriding at cathodic potential [1, 2]. Current work on the use of the active screen, mainly in glow-discharge nitriding, focuses on studying: the structure and properties of the layers formed in relation to the technological parameters [3, 4] or the influence of the size and distance of the processed workpieces from the walls of the active screen [5 – 7]. Glow-discharge treatment at plasma potential using an active screen has also found application in the processes of carburizing and nitrocarburizing [8, 9] and in the surface modification of polymers [10, 11]. A very important, common feature of this techniqus is full control of the microstructure, chemical and phase composition, thickness, and the surface topography of the layers formed [1 – 3]. In a series of tests carried out and described in articles on glow-discharge nitriding processes, there is no mention of any comparison conducted to assess the effect of the active screen on the properties of the diffusion layer formed on steel elements processed at cathodic potential and at plasma potential where the workpiece is isolated from the cathode.

The aim of the work was to compare microstructure, (surface morphology, roughness, chemical and phase composition) and properties (hardness, wear resistance, coefficient of friction and corrosion resistance) of nitrided layers produced in three processes: in classical glow-discharge nitriding at cathodic potential, at plasma potential with an active screen and at cathodic potential also using an active screen, all of which were modified by changing the nature of the current applied. Each of the processes was carried out using DC glow-discharge and pulsed discharge on single-phase austenitic X2CrNiMo17-12-2 (AISI 316L) steel, which is commonly used in the medical and chemical industries.

2. TEST METHODOLOGY

Austenitic X2CrNiMo17-12-2 (AISI 316L) stainless steel with the following chemical composition expressed in wt.%, was used in the study: C < 0.03, Si < 0.08, Mn < 2, P < 0.045, S < 0.03, Cr 16 – 18, Mo 2 – 2.5, Ni 12 – 15, the rest being Fe. The samples used in the study were cut out from a rod and had a diameter of 25 mm and a thickness of 6 mm. The flat surfaces tested were ground using 240, 400 and 800-grit sandpaper.

The nitrided layers were produced on the austenitic steel in 6 technological variants using the same basic parameters, i.e. a process temperature of 440°C, working chamber pressure of 200 Pa, nitrogen to hydrogen mixture ratio of 1:1, process time 21.6 ks. The processes were assisted thermally by using a so-called hot anode, which was heated by means of heaters to 400 °C. The layers were produced in a classical nitriding process at cathodic potential (CP), at plasma potential using an active screen (ASPP) where the processed workpiece was isolated from the cathode, and at cathodic potential with an active screen (ASCP) (Fig. 1). The processes were carried out in conditions of DC glow-discharge (CP-DC, ASPP-DC, ASCP-DC) and pulsed glow-discharge (CP-Pulse, ASPP-Pulse, ASCP-Pulse) at a frequency of 100 kHz and a pulse dead time (PDT) of 2 μs.

* Corresponding author. Tel.: +48 22 234 87 02, fax: +48 22 234 85 14
E-mail address: *borowski.tomasz@wp.pl* (T. Borowski)

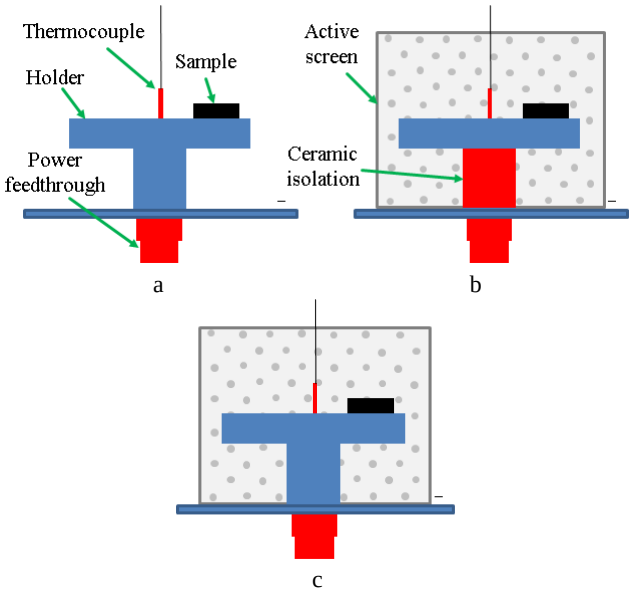

Fig. 1. Glow-discharge process technology diagrams: at cathodic potential (CP) (a), at plasma potential (ASPP) (b), at cathodic potential using an active screen (ASCP) (c)

Examinations of the cross-section microstructure of the nitrided layers produced were performed using an optical Nikon Eclypse LV150N microscope. Studies of the morphology of the surface of the layers and the chemical composition was carried out using a Hitachi S-3500N scanning electron microscope equipped with a Thermo NORAN VANTAGE X-ray Energy Dispersive Spectrometer (EDS). The roughness of the surface of the layers was measured by means of the contact method, for which a Mitutoyo SJ-210 device was used. Hardness was measured on the surface of the layers produced under a load of 50 g (HV0.05) using a ZWICK micro-hardness meter. XRD patterns were taken with a Bruker D8 ADVANCE diffractometer using filtered Cu Kα ($\lambda = 0.154056$ nm) radiation at room temperature. The recording conditions of the XRD patterns were as follows: voltage 40 kV, current 40 mA, angular range 2Θ from 28° to 60°, step Δ2Θ – 0.05°, counting time – 3 s. The XRD patterns were analysed using Brucker EVA software.

Resistance to wear by friction was tested using a T-21 ITEE Radom tribotester employing the "ball-on-disc" method in accordance with the requirements set out in the standards ASTM G 99-05, ISO 20808:2004, at ambient temperature (approximately 22 ± 2°C) and a relative humidity of 45 %. 10 mm Al_2O_3 ceramic balls with a polished surface were used in the tests, which were carried out at a load of 10 N, a sliding velocity 0.105 m/s, a friction radius of 8 mm, and the measurements were performed for 5000 rotations. Before each measurement, the surface of the ball placed in the fixture was degreased in acetone. The wear tracks formed on the samples were analysed using an optical microscope.

The corrosion resistance of AISI 316L stainless steel before and after glow-discharge nitriding was tested in a 0.5 M not deoxidised NaCl sodium chloride solution. A three-electrode system was used in the tests, in which the sample constituted the test electrode, a saturated calomel electrode (SCE) was the reference electrode, and a platinum grid was used as the auxiliary electrode. Before the tests, the materials were kept in the measurement system for 2 hours, which allowed their corrosion potentials to stabilise and their corrosive values to be determined. Afterwards, the polarisation resistance was examined using the Stern method by polarising the test material from values of 10 mV lower to 10 mV higher from the designated corrosion potential with a potential sweep rate of 0.2 mV/sec. The R_{pol} polarisation resistance was determined based on the inclination of the slope of the calculated $E = f(i)$ dependence. The potentiodynamic method was then used to register the anodic polarisation curves of the test materials. The samples were polarised from a potential of 200 mV lower than the corrosion potential up to a potential of 1500 mV. A potential sweep rate of 0.2 mV/sec was used in the potential range of ± 200 mV from the corrosion potential. A rate of 0.8 mV/sec was used in the remaining potential range. E_{pit} pitting corrosion potentials were determined for the test materials based on the polarisation curves obtained. The i_{cor} corrosion current density and the E_{cor} corrosion potential were determined by means of Tafel plots in the scope of applicability of this method.

3. RESULTS

Fig. 2 shows the cross-section microstructures of the produced nitrided layers. As can be seen, their thicknesses differ only slightly between each other. The nitrided layer formed in DC glow-discharge at cathodic potential (CP-DC) had a thickness of 7.1 µm, the layer produced at plasma potential (ASPP-DC) showed a thickness of 5.4 µm, while the layer produced at cathodic potential using an active screen (ASCP-DC) showed a thickness of 5.8 µm. The thicknesses of the nitrided layers produced under pulsed glow-discharge conditions amounted to 5.5 µm (CP-Pulse), 5 µm (ASPP-Pulse) and 6.1 µm (ASCP-Pulse) respectively.

Fig. 3 shows the surface morphology of the nitrided layers formed, as seen under an SEM electron microscope. It can be observed that the nitriding processes resulted in significant changes to the surface of the steel (Fig. 3 b – g), compared to the surface of the material in its initial state (Fig. 3 a).

Small amounts of precipitation were observed on the surface of the nitrided layers, the least of which were found in layers nitrided at plasma potential (ASPP) (Fig. 3 c – f), while the most were found in layers glow-discharge nitrided at cathodic potential (CP) (Fig. 3 b – e). The impact of the applied DC discharge or pulsed discharge on the formation of small amounts of precipitates is also visible. After application of pulsed glow-discharge, fewer small precipitates can be seen on the surface of the nitrided steel (Fig. 3 e, f, g) than in the case of layers produced under DC discharge conditions (Fig. 3 b, c, d). It should be noted that these precipitates were not identified in XRD examinations, which could mean that they are very small and their thickness on the surface of the layer is in the order of a few dozen nanometres.

Observations of the morphology of the nitrided layers' surfaces are reflected in the values of surface roughness. Each nitriding process leads to a development of the surface of austenitic steel (Table 1).

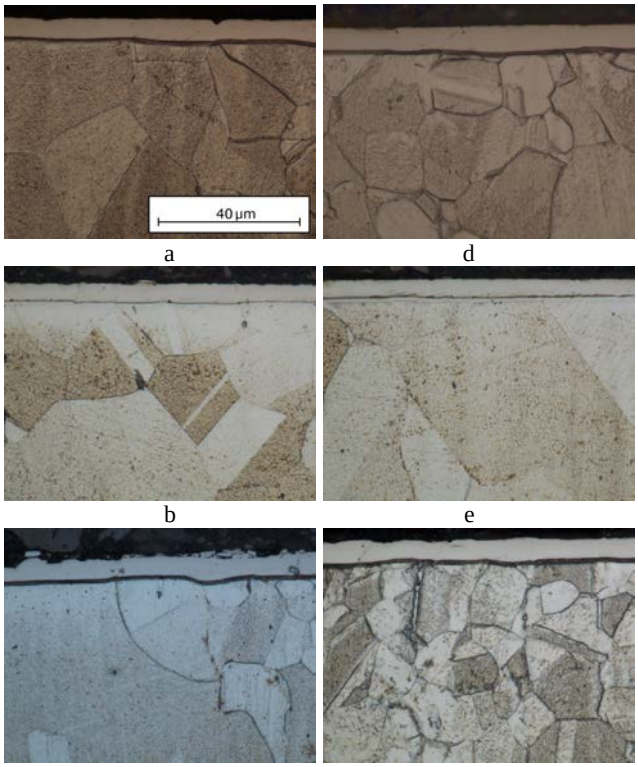

Fig. 2. The microstructure of the nitrided layers produced at cathodic potential (a), at plasma potential (b), at cathodic potential with the use of an active screen (c) in DC glow-discharge conditions and the respective microstructures of the layers produced under pulsed current conditions (d, e, f) – magnification 1000x

Table 1. Surface roughness parameters of austenitic steel and nitrided layers

Parameter / Sample	*R*a, µm	*R*q, µm	*R*z, µm
AISI 316L	0.041	0.053	0.291
CP-DC	0.070	0.089	0.429
CP-Pulse	0.066	0.083	0.383
ASPP-DC	0.060	0.076	0.390
ASPP-Pulse	0.052	0.067	0.347
ASCP-DC	0.117	0.145	0.756
ASCP-Pulse	0.086	0.108	0.523

The lowest roughness (*R*a = 0.052 µm) is found in the layers produced in active screen pulsed plasma potential nitriding (ASPP-Pulse). In turn, the highest roughness (*R*a = 0.117 µm) was found on the surfaces of layers formed in the active screen cathodic potential process under DC discharge conditions (ASCP-DC). It can be observed that processes carried out under pulsed discharge conditions lead to the formation of layers with lower surface roughness compared to processes carried out under DC conditions (Table 1).

Nitrided layers produced on steel with a γ austenite structure are characterized by a single phase structure consisting of γ_N nitrogen austenite, also known as the *S* phase [12]. During the process of nitriding at 440°C, γ austenite with a regular face-centered cubic structure is transformed into γ_N nitrogen austenite with a tetragonal structure. A precise determination of the type of the unit cell being formed in the lattice is very difficult [12].

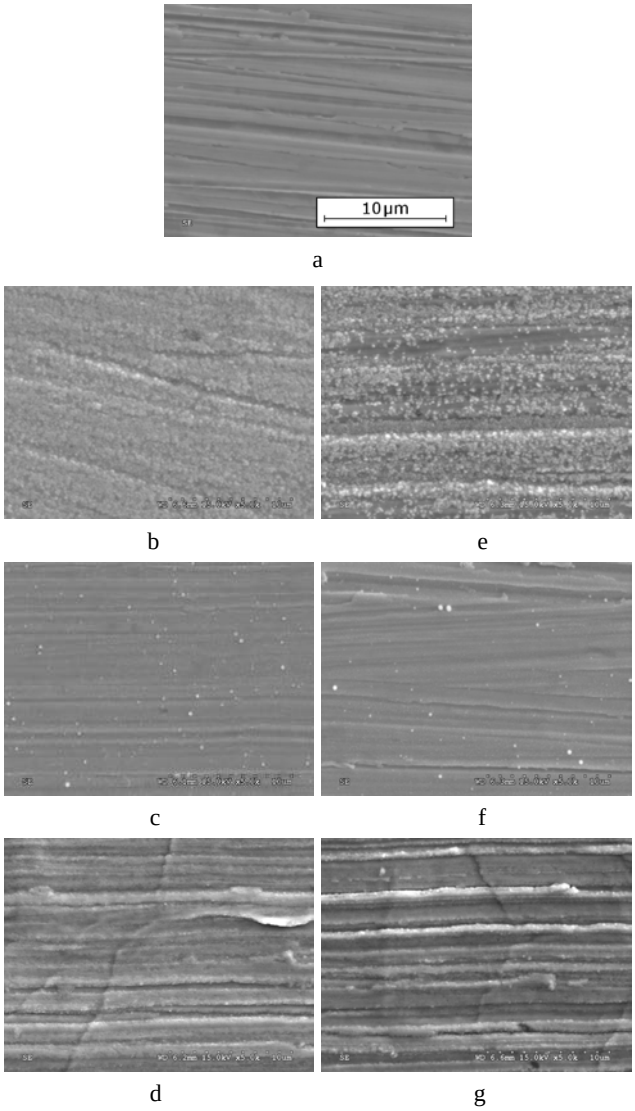

Fig. 3. Surface morphology of steel in initial state (a) and of nitrided layers produced in the following processes: at cathodic potential (b), at plasma potential (c), at cathodic potential assisted by an active screen (d) under DC discharge conditions and the respective morphologies of the layers produced under pulsed discharge (e, f, g) – magnification 5000x.

Fig. 4 presents sample XRD patterns for layers nitrided at cathodic potential with the use of an active screen under DC and pulsed glow-discharge conditions. It can be observed that the nitrided layer is made only from the *S* phase. Peaks with a very low intensity are observed starting from the γ phase, which originates in the substrate, as the depth of penetration of the X-ray beam may be slightly greater than the thickness of the layers. In the nitrided layers, peaks are not visible from phase CrN onwards, the formation of which (usually at a temperature of > 450 °C) leads to a segregation of chromium at grain boundaries and formation of anode areas with a depleted concentration of chromium (<13 % wt), which ultimately results in a reduction of corrosion resistance [4]. For each nitrided layer, peaks are located elsewhere from the *S* phase onwards along the 2Θ axis, which is associated with a different nitrogen concentration in each of the nitrided layers produced, and which is also reflected in the measured d_{hkl} interplanar spacings. The smaller the 2Θ

angle, where the peak of the *S* phase is located, the greater the d_{hkl} parameter and the greater the concentration of nitrogen in the nitrided layer (Table 2) The d_{hkl} parameters were determined for the *S* phase planes (111) and (200). The lowest d_{hkl} parameter value and nitrogen concentration was recorded for the steel nitrided in active screen plasma potential (ASPP), whereas the highest d_{hkl} parameter value and the highest nitrogen concentration was recorded for the steel nitrided in active screen cathodic potential (ASCP). In the case of the application of pulsed discharge, in all cases there is a reduction in the value of the d_{hkl} parameter (lower concentration of nitrogen) compared to the layers produced under DC discharge conditions.

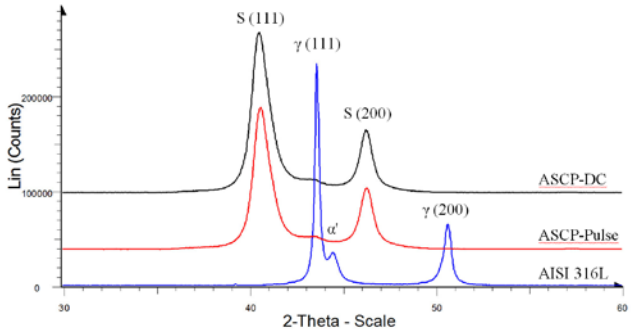

Fig. 4. XRD patterns of austenitic steel and nitrided layers obtained in active screen cathodic potential nitriding under DC and pulsed discharge

Table 2. d_{hkl} interplanar spacings of the S phase and the concentration of nitrogen in the nitrided layers formed

Parameter / Sample	d_{111}, nm	d_{200}, nm	N, wt %
AISI 316L	0.2076	0.1802	-
CP-DC	0.2194	0.1960	1.97
CP-Pulse	0.2183	0.1957	1.77
ASPP-DC	0.2183	0.1941	1.33
ASPP-Pulse	0.2182	0.1947	1.17
ASCP-DC	0.2228	0.1963	2.57
ASCP-Pulse	0.2221	0.1961	2.36

The XRD patterns of austenitic steel (Fig. 4), in addition to the peaks of the γ phase, reveal an additional peak at an angle of ca. 2Θ = 44.5°. It corresponds to the body-centred cubic structure formed from the partial transformation of austenite. In the process of sample surface grinding, a thin layer of α'_d deformation martensite appeared on the surface of the steel as a result of cold work. This additional peak corresponds directly to the body-centred cubic structure of martensite. In the process of nitriding, the α'_d deformation martensite is transformed into α'_N nitrogen martensite and then into γ_N nitrogen austenite, that is why α'_d martensite is no longer seen in the nitrided layers. This mechanism has been precisely defined in a separate publication, in which metastable high-nickel content austenite was studied [13].

Based on the hardness measurements it can be observed that each of the glow-discharge nitriding processes increases the hardness of the surface of AISI 316L austenitic steel (Tab. 3) The highest hardness values, i.e. 1355 HV0.05 were recorded for the layers which were nitrided in the active screen cathodic potential process under pulsed discharge conditions (ASCP-Pulse). In turn, the lowest hardness of all the layers was recorded in the ASPP-Pulse and ASPP-DC processes, where it reached a level of ca. 900 HV0.05. It can be observed that the layers produced in pulsed discharge are characterized by a higher hardness than the layers formed in DC discharge conditions, which is particularly visible in layers nitrided at cathodic potential (CP) and in active screen cathodic potential nitriding (ASCP). The differences in hardness range from 100 to 150 HV0.05. The results obtained are different from those expected, because the layers nitrided in pulsed discharge conditions are characterized by a lower concentration of nitrogen than in the case of layers nitrided in DC conditions (Table 2).

Table 3. Hardness of austenitic steel and nitrided layers

Parameter / Sample	HV0.05
AISI 316L	296
CP-DC	1023
CP-Pulse	1121
ASPP-DC	893
ASPP-Pulse	906
ASCP-DC	1205
ASCP-Pulse	1355

Measurements of the formed layers' resistance to wear by friction were made using the "ball-on-disc" method at a load of 10N. The method measures such values as the width of the wear track and the friction coefficient (Fig. 5). Almost all the glow-discharge nitriding processes improve the austenitic steel's resistance to wear by friction (Fig. 5 a). The μ coefficients of friction of the produced layers and of steel in initial state were at a very similar level and equalled a value of ca. 0.7 (Fig. 5 b). ASPP-Pulse layers, despite a relatively low hardness (906 HV0.05) and ASCP-Pulse layers showed by large the lowest wear levels (Fig. 5 a). Surprisingly, relatively high wear values were recorded for layers nitrided at cathodic potential (CP-DC, CP-Pulse) and for layers nitrided at active screen cathodic potential under DC glow-discharge conditions (ASCP-DC). These layers were characterised by about a 4-fold greater hardness compared to the initial state, however, the deciding factor for the rapid wear of layers with a thickness of 5 – 7 μm could have been a high level of their surface development (Table 1).

Fig. 6 presents the anodic polarization curves of austenitic steel in initial state and of the nitrided layers formed on the steel, whereas Table 4 shows the designated E_{cor} corrosion potential values, the i_{cor} corrosion current densities, R_{pol} polarisation resistance values and E_{pit} pitting potentials.

All the glow-discharge nitriding processes increased the resistance of AISI 316L stainless steel to pitting corrosion, as evidenced by a shift of the E_{pit} pitting potentials from 320 mV for the material in initial state up to a value of over 1150 mV for the nitrided layers (Table 4). In addition, for the layer formed at plasma potential under pulsed discharge conditions (ASPP-Pulse), no pitting potential was recorded in the entire potential range. However, the value of anodic currents in the passive state for most of the nitrided layers (i.e. produced in ASPP and CP processes) are higher than the current densities of the passive state for AISI 316L steel in initial state (Fig. 6). Only processes carried out by means of active screen

cathodic potential nitriding (ASCP processes) lead to the formation of nitrided layers characterised by anode current densities, which in the passive state are lower than those characteristic for AISI 316L steel (Fig. 6).

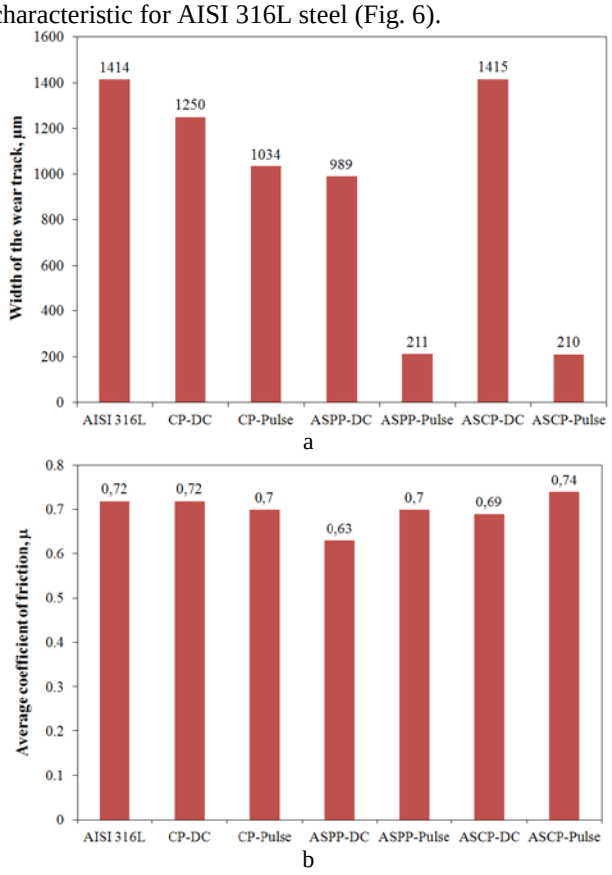

Fig. 5. Wear widths (a) and friction coefficients (b) of layers nitrided at cathodic potential, at plasma potential and in active screen cathodic plasma nitriding in DC and pulsed glow-discharge conditions

It is worth noting that the passive layers formed on the nitrided layers undergo transformation in the course of potentiodynamic testing, as evidenced by the presence of trans-passive peaks on the polarisation curves. One trans-passive peak was registered at a potential of ca. 650 mV for the nitrided layers with the highest concentration of nitrogen (ASCP-DC and ASCP-Pulse). Nitrided layers produced in CP-DC, CP-Pulse and ASPP-DC processes are characterized by the presence of two trans-passive peaks at different potentials, while the second peak appears at a potential of ca. 1000 mV. Nitriding at active screen plasma potential in pulsed discharge conditions (ASPP-Pulse) leads to the formation of a nitrided layer, which in the passive state does not undergo trans-passive transformation.

Nitrided layers with the highest nitrogen content in *S* phase (ASCP) are characterised by the best corrosion resistance. Glow-discharge nitriding at cathodic potential assisted by an active screen helps in obtaining nitrided layers, whose corrosion potential and polarisation resistance values are higher, while the corrosion current density values are comparable to those characteristic for AISI 316L steel in initial state (Table 4). Also, only these layers are characterised by anodic current densities which are lower than the values recorded for the substrate material (Fig. 6). The other nitrided layers (CP, ASPP) are characterized by much lower corrosion potential and polarisation resistance values and comparable or higher corrosion and anodic current densities than for AISI 316L steel in initial state (Fig. 6, Table 4).

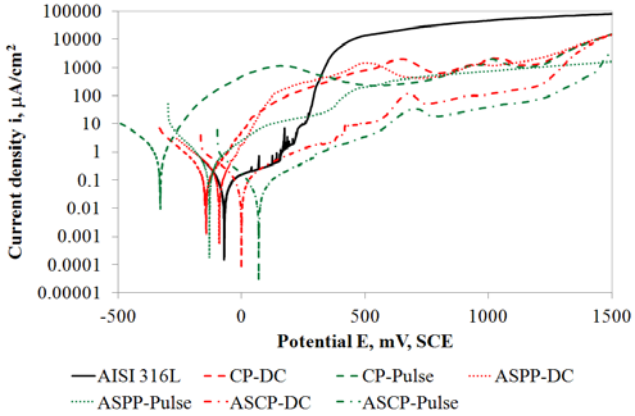

Fig. 6. Polarisation curves of AISI 316L steel and the nitrided layers formed

Table 4. Characteristic electrochemical parameters of AISI 316L steel and the nitrided layers of AISI 316L steel and the nitrided layers formed determined by means of the potentiodynamic method

Parameter / Sample	E_{cor}, mV	i_{cor}, µA/cm²	R_{pol}, kΩ·cm²	E_{pit}, mV
AISI 316L	-70	0.08	231	320
CP-DC	-145	0.18	91	1150
CP-Pulse	-330	0.91	13	1150
ASPP-DC	-91	0.09	47	1250
ASPP-Pulse	-131	0.47	68	>1500
ASCP-DC	+1	0.09	265	1250
ASCP-Pulse	+70	0.07	403	1425

Use of pulsed plasma nitriding at plasma potential (ASPP-Pulse) and at cathodic potential (CP-Pulse) reduces the corrosive properties (E_{cor}, i_{cor}) of the nitrided layers as compared to the layers produced under DC discharge conditions (ASPP-DC, CP-DC). In the case of active screen nitriding at cathodic potential, the impulse plasma (ASCP-Pulse) makes it possible to obtain nitrided layers with better characteristics compared to those produced under DC discharge conditions (ASCP-DC).

4. DISCUSSION AND CONCLUSIONS

The glow-discharge nitriding techniques used made it possible to modify the surface layers of AISI 316L austenitic steel by improving their resistance to wear by friction and their corrosion resistance. In 6 different nitriding processes: at cathodic potential (CP), at plasma potential (ASPP) and at cathodic potential with the use of an active screen (ASCP) under DC and pulsed glow-discharge conditions, layers 5 to 7 µm thick were obtained, made only of γ_N nitrogen austenite (*S* phase), in which the various layers varied in terms of their d_{hkl} interplanar spacings and thus also by the nitrogen content. Each of the processes used made it possible to obtain nitrided layers with different nitrogen concentrations ranging from 1.2 to 2.6 wt.%, which in turn determined the hardness values of the layers. Unfortunately, a clear correlation between the hardness of the nitrided layers and their resistance to wear by friction was not observed. In the

case of complete wear of nitrided layers with a relatively low thickness (5 – 7 μm), the quality of the surface, which undergoes testing, is of crucial importance. In this case, it can be stated that the layer which was nitrided at plasma potential in pulsed discharge conditions (ASPP-Pulse), is characterized by the best resistance to wear by friction. The surface of the layer was the least developed (Ra = 0.052 μm) and had one of the lowest hardness values (906 HV0.05). A similar level of wear is presented by the layer which was nitrided at cathodic potential using an active screen in pulsed discharge conditions (ASCP-Pulse), which, in turn, is characterized by the highest hardness value (1355 HV0.05) and a roughness of Ra = 0.086 μm. Therefore, it can be concluded that resistance to wear by friction of diffusion layers produced on austenitic steel depends on a combination of factors such as the degree of development of the surface and the level of hardness.

Glow-discharge nitriding processes make it possible to obtain different nitrided layers with better resistance to pitting corrosion as compared to the substrate material. The best corrosion properties are demonstrated by nitrided layers produced in active screen glow-discharge nitriding at cathodic potential (ASCP), as they are characterised by the highest E_{cor} corrosion potentials, i_{cor} corrosion density values which are close to the values of the steel in initial state, and one of the highest E_{pit} pitting potentials (beginning of pitting corrosion). In active screen glow-discharge nitriding at cathodic potential, the application of a pulsed discharge made it possible to obtain nitrided layers with even better properties.

By analysing the impact of DC and pulsed discharge, it can be concluded that they are of great importance in the process of shaping the properties of austenitic steel. Application of pulsed glow-discharge with a pulse frequency of 100 kHz contributes to reducing the roughness of the nitrided layers and to increasing their hardness as compared to the layers produced under DC discharge conditions. It was also noted that the layers produced under pulsed discharge conditions have a lower concentration of nitrogen and a lower d_{hkl} parameter value, which has an opposite impact on the results of hardness measurements than expected. The formation of nitrided layers with lower surface roughness and higher surface hardness under pulsed glow-discharge conditions contributes to an improvement in the resistance to wear by friction. When analysing corrosion resistance, it can be concluded that the layers produced under pulsed discharge conditions have a better resistance to pitting corrosion (higher E_{pit} value) compared to the layers produced under DC current.

The proposed methods of glow-discharge nitriding show how greatly the properties of austenitic steel can be improved. Based on the preliminary tests carried out in this work, it can be concluded that the method of active screen pulse glow-discharge nitriding at cathodic potential (ASCP-Pulse) is the most promising, as it provides the highest increase in hardness, in resistance to wear by friction and a very significant increase in the corrosion resistance of AISI 316L austenitic steel exposed to a chloride environment. It is very important to examine the mechanisms that affect the strengthening of the top layer in the process of nitriding under pulse discharge conditions. In the near future, the authors also wish to examine the effect of other steel structures (martensitic or ferritic grades) on the properties of nitrided layers produced in the 6 variants presented.

Acknowledgments

The project was funded by the National Science Center based on decision No. DEC-2012/07/D/ST8/02599.

REFERENCES

1. **Alves Jr., C., de Araújo, F.O., Ribeiro, K.J.B., et al.** Use of Cathodic Cage in Plasma Nitriding *Surface & Coatings Technology* 201 2006: pp. 2450 – 2454. http://dx.doi.org/10.1016/j.surfcoat.2006.04.014
2. **Ribeiro, K.J.B., de Sousa, R.R.M., de Araújo, F.O., et al.** Industrial Application of AISI 4340 Steels Treated in Cathodic Cage Plasma Nitriding Technique *Materials Science and Engineering* A 479 2008: pp. 142 – 147.
3. **Ahangarani, Sh., Mahboubi, F., Sabour, A.R.** Effects of Various Nitriding Parameters on Active Screen Plasma Nitriding Behavior of a Low-Alloy Steel *Vacuum* 80 2006: pp. 1032 – 1037.
4. **Li, C.X., Bell, T.** Corrosion Properties of Active Screen Plasma Nitrided 316 Austenitic Stainless Steel *Corrosion Science* 46 2004: pp. 1527 – 1547. http://dx.doi.org/10.1016/j.corsci.2003.09.015
5. **de Sousa, R.R.M., de Araújo, F.O., Ribeiro, K.J.B., et al.** Cathodic Cage Nitriding of Samples with Different Dimensions *Materials Science and Engineering* A 465 2007: pp. 223 – 227.
6. **de Sousa, R.R.M., de Araújo, F.O., da Costa, J.A.P., et al.** Nitriding in Cathodic Cage of Stainless Steel AISI 316: Influence of Sample Position *Vacuum* 83 2009: pp. 1402 – 1405.
7. **Nishimoto, A., Nagatsuka, K., Narita, R., et al.** Effect of the Distance Between Screen and Sample on Active Screen Plasma Nitriding Properties *Surface & Coatings Technology* 205 2010: pp. S365 – S368.
8. **de Sousa, R.R.M., de Araújo, F.O., Barbosa, J.C.P.** Nitriding Using Cathodic Cage Technique of Austenitic Stainless Steel AISI 316 with Addition of CH_4 *Materials Science and Engineering* A 487 2008: pp. 124 – 127. http://dx.doi.org/10.1016/j.msea.2007.10.001
9. **Corujeira Gallo, S., Dong, H.** Study of Active Screen Plasma Processing Conditions for Carburising and Nitriding Austenitic Stainless Steel *Surface & Coatings Technology* 203 2009: pp. 3669 – 3675.
10. **Li, C.X., Bell, T.** Potential of Plasma Nitriding of Polymer for Improved Hardness and Wear Resistance *Journal of Materials Processing Technology* 168 2005: pp. 219 – 222.
11. **Fu, X., Jenkins, M.J., Sun, G.** Characterization of Active Screen Plasma Modified Polyurethane Surfaces *Surface & Coatings Technology* 206 2012: pp. 4799 – 4807.
12. **Christiansen, T., Somers, M.A.J.** On the Crystallographic Structure of S-phase *Scripta Materialia* 50 2004: pp. 35 – 37.
13. **Borowski, T., Jeleńkowski, J., Psoda, M., Wierzchoń, T.** Modifying the Structure of Glow Discharge Nitrided Layers Produced on High-nickel Chromium-less Steel with the Participation of an Athermal Martensitic Transformation *Surface & Coatings Technology* 204 2010: pp. 1375 – 1379.